

## Effect of Solution Annealing on Austenite Morphology and Pitting Corrosion of Super Duplex Stainless Steel UNS S 32750

Changwon Sung<sup>1</sup>, Byung-Hyun Shin<sup>2,\*</sup>, Wonsub Chung<sup>2,\*</sup>

<sup>1</sup> Kowel corporation, Yangsan, Korea

<sup>2</sup> School of Materials Science and Engineering, Pusan National University, Busan 46241, Republic of Korea

\*E-mail: [lemonhouse@pusan.ac.kr](mailto:lemonhouse@pusan.ac.kr), [wschung1@pusan.ac.kr](mailto:wschung1@pusan.ac.kr)

Received: 2 April 2021 / Accepted: 12 May 2021 / Published: 30 June 2021

---

The pitting corrosion resistance of super duplex stainless steel (SDSS) varies depending on heat-treatment conditions. Therefore, in this study, the volume fraction and morphology of austenite on SDSS were controlled in 6 samples, and the effect on the pitting corrosion after solution annealing was analyzed to of the critical pitting temperature (CPT). The pitting-resistance equivalent (PRE = wt % Cr + 3.3 wt % Mo + 16 wt % N) was became equal by solution annealing, but the CPT exhibited varying values. Despite heat treatment of the solution annealing, the CPT increased by 15.9 °C from 67.5 °C to 83.4 °C. The solution annealing removed the segregation of the chemical composition and assisted in improving the PRE; however, it not removed in a non-uniform morphology of austenite. Therefore, the corrosion resistance of SDSS can be optimized by appropriately controlling the morphology of austenite during the manufacturing process.

---

**Keywords:** Solution annealing, Austenite morphology, Volume fraction, Pitting corrosion, Super duplex stainless steel.

### 1. INTRODUCTION

Materials used in offshore plant and chemical refinery industries operate in seawater and under high pressures; therefore, they require high corrosion resistance and strength [1-2]. Super duplex stainless steel (SDSS), or dual-phase stainless steel with austenite and ferrite phases is proper for application in various materials that are used in such high-pressure environments because of its high corrosion resistance and strength. However, the pitting corrosion resistance of SDSS is dependent on heat-treatment conditions. Previous studies on SDSS show mechanical and electrochemical properties at a specific temperature range [1-22].

The austenite morphology changes in manufacturing processes, such as casting and forging. A casted microstructure has a non-uniform austenite morphology, and a forged microstructure has a directionality that is based on the forging direction [12-16]. Even when heat treatment is performed on the solution annealing, the two materials exhibit different corrosion resistances. However, because previous research has been focused on the effects of the heat-treatment temperature and operating temperature, research on the dependency of the morphology of austenite on manufacturing processes have not been conducted.

The properties of SDSS under specific heat-treatment conditions were investigated in previous studies [3-22]. Nillson studied the effect of the heat-treatment temperature on the austenite morphology and not its effect on the pitting corrosion [3]. Chen studied the effect of solution annealing from 1030 °C to 1120 °C but only focused on the effect of solution annealing temperature [5]. Shin studied the effect of heat-treatment conditions, excluding its effect on austenite growth [15]. Park studied the dependencies of the austenite morphology but did not consider austenite growth as well [21]. They all did not study the effects of solution annealing on the volume fraction and morphology of austenite as well as the pitting corrosion.

In this study, the effect of the heat treatment on the volume fraction and morphology of austenite and pitting corrosion (one of electrochemical property) of SDSS was investigated. The effects of the heat-treatment were examined using field emission scanning electron microscopy (FE-SEM). The chemical composition was calculated using energy dispersive spectroscopy (EDS) [22-30]. The pitting corrosion resistance with the control of the austenite morphology was determined using the critical pitting temperature (CPT) test [2-22].

## 2. EXPERIMENTAL METHOD

The SDSS considered had a pitting-resistance equivalent ( $PRE = \text{wt \% Cr} + 3.3 \text{ wt \% Mo} + 16 \text{ wt \% N}$ ) in the range from 40 to 50 [3-4]. The chemical composition of the SDSS used in this study is listed in Table 1. This SDSS had 25 wt % Cr and 7 wt %. UNS S32750 was initially cast. The volume fraction and morphology of austenite were controlled by heat treatment as shown in Table 2.

**Table 1.** Chemical composition of commercial UNS S32750.

	C	N	Mn	Ni	Cr	Mo	Cu	W	Fe	PRE
Chemical composition, wt %	0.01	0.27	0.79	6.8	25.0	3.8	0.18	0.02	Bal	41.9

The microstructure after heat-treatment was polished from #80 to 0.25 μm with diamond paste and etched in 20 wt % NaOH to 10 V after 10 s [14-16]. Etching causes corrosion in ferrite owing to its low, uniform corrosion resistance and low Ni content [3-4]. The volume fractions of austenite and ferrite

were obtained using an image analyzer [14-16]. The analysis results of the volume fractions were averaged with seven measurements using an image of x200. The microstructures of the specimens were examined by FE-SEM (Hitachi S-4800, Japan) to check the effects on the volume fraction and morphology [15, 16].

**Table 2.** Heat-treatment conditions to control the volume fraction and morphology of austenite in super duplex stainless steel UNS S32750.

Heat treatment condition			
# a	Casting	# a, SA	Casting → 1100 °C
# b	Casting → 1000 °C	# b, SA	Casting → 1000 °C → 1100 °C
# c	Casting → 1100 °C	# c, SA	Casting → 1100 °C → 1100 °C
# d	Casting → 1300 °C → 900 °C	# d, SA	Casting → 1300 °C → 900 °C → 1100 °C
# e	Casting → 1300 °C → 1200 °C	# e, SA	Casting → 1300 °C → 1200 °C → 1100 °C
# f	Casting → 1300 °C → 1300 °C	# f, SA	Casting → 1300 °C → 1300 °C → 1100 °C

The pitting corrosion resistance of the specimens was obtained using the CPT test, which is an electrochemical test [13-21]. This test can be used to measure pitting growth. CPT was analyzed in a three-electrode cell (working electrode, reference electrode, and counter electrode) using a potentiometer. The reference electrode had a saturated calomel electrode and Pt mesh as the counter electrode. The CPT test was used to calculate the change in current density at 700 mV in an electrolyte solution of 5.85 wt% NaCl. The dissolved oxygen in the electrolyte solution was removed by bubbling 99.98% N<sub>2</sub> gas before the test [13-15]. CPT is defined as the temperature at which the current density exceeds 100  $\mu\text{A} / \text{cm}^2$  during 1 min at 700 mV.

### 3. RESULTS AND DISCUSSION

#### 3.1. Effect of solution annealing on the volume fraction and morphology of austenite

Based on the heat-treatment conditions, the SDSS exhibited changes in the volume fraction and morphology of austenite [3-4]. Fig. 1 and Fig. 2 show the volume fraction and morphology of austenite based on the heat-treatment temperature. The volume fraction of SDSS changed according to the heat-treatment conditions, and this corresponded with the results of previous studies [14-16].

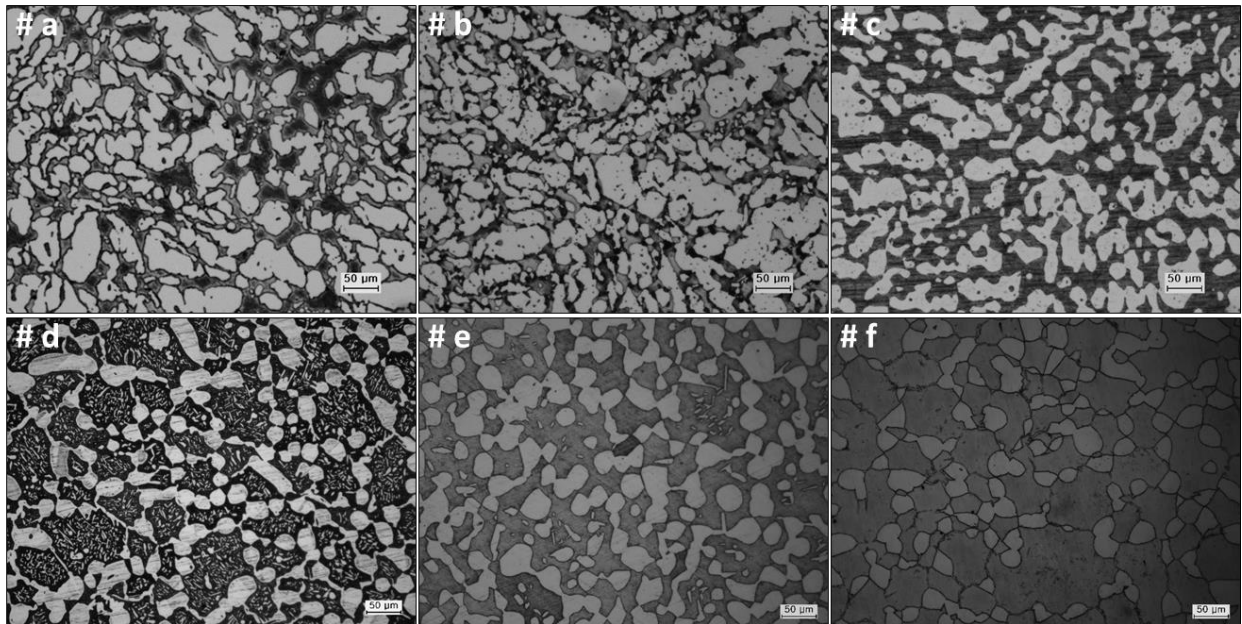


**Figure 1.** Microstructures of super duplex stainless steel UNS S3275 after heat treatment # a casting, # b casting → 1000 °C, # c casting → 1100 °C, # d casting → 1300 °C → 900 °C, # e casting → 1300 °C → 1000 °C, # e casting → 1300 °C → 1200 °C, and # f casting → 1300 °C → 1300.

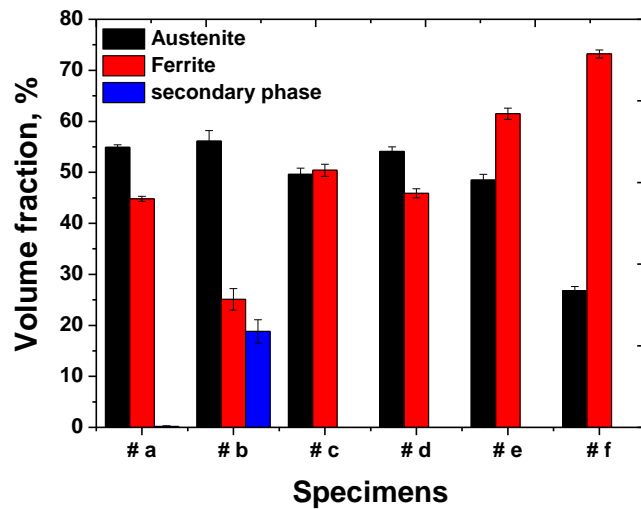


**Figure 2.** Volume fraction of super duplex stainless steel UNS S3275 after heat treatment.

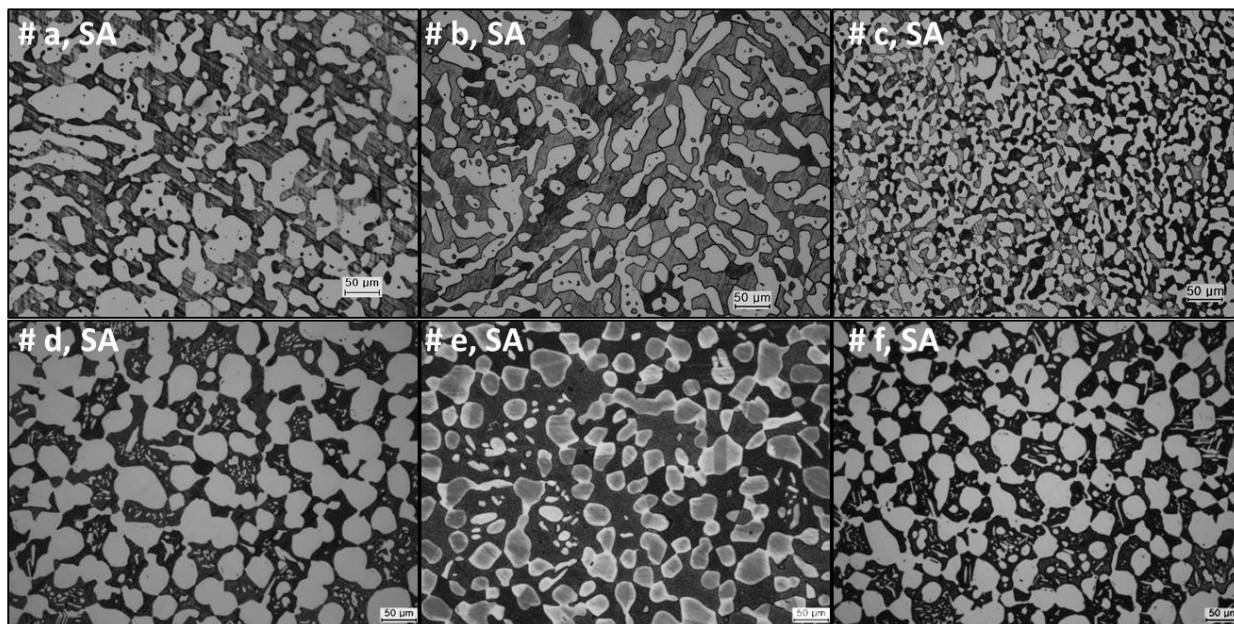


**Figure 3.** Microstructures of super duplex stainless steel UNS S32750 after solution annealing # a casting, # b casting → 1000 °C, # c casting → 1100 °C, # d casting → 1300 °C → 900 °C, # e casting → 1300 °C → 1000 °C, # e casting → 1300 °C → 1200 °C, and # f casting → 1300 °C → 1300.

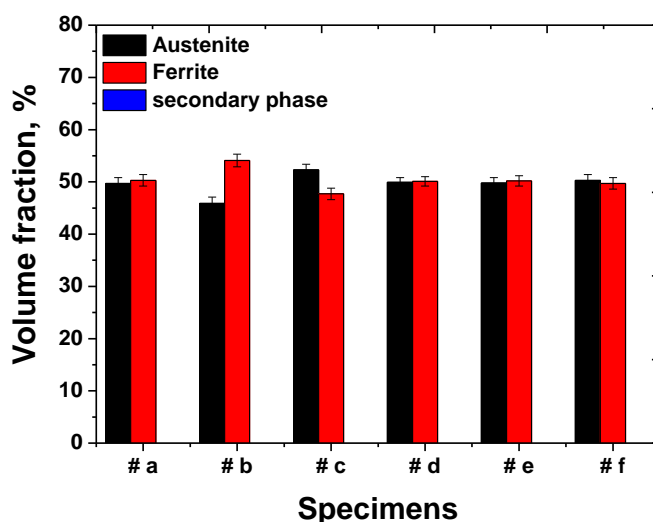


**Figure 4.** Volume fraction of super duplex stainless steel UNS S32750 after solution annealing with morphology and volume fraction of austenite.

It is known that heat treatment of a solution annealing produces an equal volume fraction and chemical composition and optimizes the corrosion resistance [3-6]. Fig. 3 and Fig. 4 show the change of the microstructure and volume fraction of austenite after solution annealing. Solution annealing resulted in equal volume fractions, but it was confirmed that the microstructure before solution annealing was affected by the process.

The effect of solution annealing is checked in the volume fractions of austenite and ferrite. Solution annealing shows in equal volume fraction of austenite and ferrite, which was consistent with the results of previous studies [14-16]. However, when 18.8% of the secondary phase was present, the volume fraction of austenite during solution annealing was reduced to 45 %.

**Table 3.** Austenite morphology before and after solution annealing of super duplex stainless steel UNS S32750.

	Austenite morphology	
	Before solution annealing	After solution annealing
# a	Heterogeneous austenite	Heterogeneous austenite
# b	Heterogeneous austenite	Heterogeneous and low fraction of austenite
# c	Combination of fine and coarse austenite	Fine austenite under 10 um
# d	Lined austenite and coarse austenite	Combination of fine under 3 um and coarse over 40 um of austenite
# e	Homogeneous but low fraction of austenite	Homogeneous austenite
# f	Homogeneous but low fraction of austenite	Combination of fine under 3 um and coarse over 30 um austenite

Solution annealing affected the morphology of austenite, as shown in Table 3. The austenite morphology affected the microstructure before solution annealing and this was identified in the various sizes and morphologies.

### 3.2. Effect of volume fraction and morphology of austenite on the pitting corrosion resistance

The pitting of stainless steel is highly influenced by its chemical composition of Cr, Mo, and N, which are known to be optimized after solution annealing [3-16].

**Table 4.** Chemical composition and volume fraction and morphology of austenite with and without solution annealing of super duplex stainless steel UNS S32750.

Chemical composition, wt. %		Cr	Mo	Ni	N	Fe	PRE
# a	Austenite	23.6	2.9	7.9	0.44	Bal	40.3
	Ferrite	26.3	4.5	5.0	0.05	Bal	41.9
# a, SA	Austenite	23.8	2.9	7.4	0.51	Bal	41.7
	Ferrite	25.6	4.5	5.5	0.05	Bal	41.4
# b	Austenite	23.3	2.9	8.0	0.42	Bal	39.7
	Ferrite	26.3	4.0	4.6	0.05	Bal	40.3
# b, SA	Austenite	23.3	2.8	7.5	0.54	Bal	41.2
	Ferrite	26.2	4.2	5.3	0.05	Bal	40.8

# c	Austenite	23.4	3.2	8.5	0.50	Bal	42.0
	Ferrite	25.9	4.5	5.9	0.05	Bal	41.6
# c, SA	Austenite	2.55	2.9	7.9	0.49	Bal	43.0
	Ferrite	26.3	4.5	4.9	0.05	Bal	41.9
# d	Austenite	23.6	2.9	7.9	0.53	Bal	41.7
	Ferrite	26.3	4.5	5.0	0.05	Bal	41.9
# d, SA	Austenite	23.4	3.2	8.5	0.51	Bal	42.1
	Ferrite	25.9	4.5	5.9	0.05	Bal	41.6
# e	Austenite	23.3	2.9	7.5	0.62	Bal	42.7
	Ferrite	26.0	4.9	5.4	0.05	Bal	40.3
# e, SA	Austenite	23.4	3.2	8.5	0.51	Bal	42.1
	Ferrite	25.9	4.5	5.9	0.05	Bal	41.6
# f	Austenite	23.5	3.0	7.6	0.71	Bal	44.6
	Ferrite	25.6	4.0	5.3	0.05	Bal	39.5
# f, SA	Austenite	23.4	3.2	8.5	0.51	Bal	42.1
	Ferrite	25.9	4.5	5.9	0.05	Bal	41.5

This study confirmed the chemical composition of austenite and ferrite. The chemical composition of austenite and ferrite is presented in Table 4. The PRE (= wt % Cr + 3.3 wt % Mo + 16 wt % N) of each phase was calculated using Cr, Mo, and N [3-5, 13-16]. The PRE varied, depending on the volume fraction of austenite; however, it was leveled after solution annealing. The difference of PRE between austenite and ferrite is shown in Fig. 5. After solution annealing, the difference in the PRE decreased to 1 or less. However, # C increased the difference in PRE after solution annealing. This difference in PRE affects pitting corrosion, which can be confirmed by CPT.

$$\text{Difference of PRE} = |\text{austenite PRE} - \text{ferrite PRE}|$$

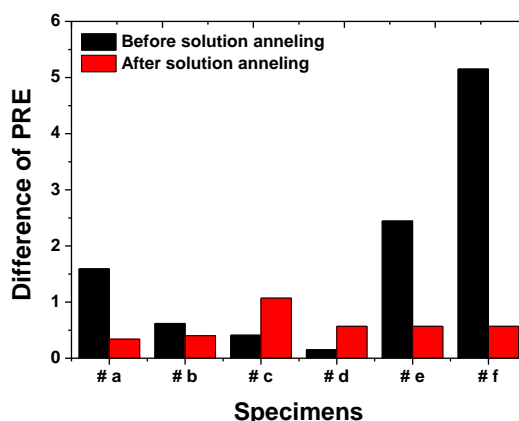


**Figure 5.** Gap of PRE with volume fraction and morphology of austenite in super duplex stainless steel UNS S32750.

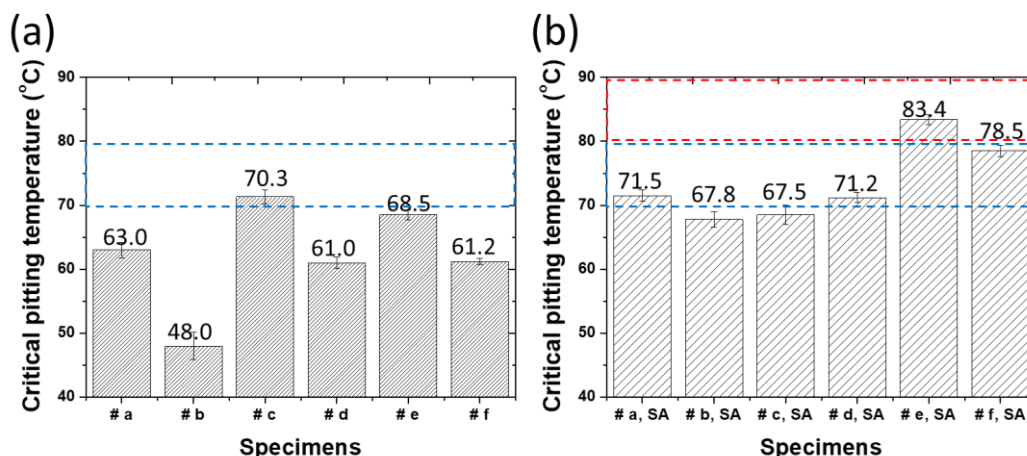


**Figure 6.** CPT with volume fraction and morphology of austenite in super duplex stainless steel UNS S32750 (a) before solution annealing, and (b) after solution annealing.

The morphology and volume fraction of austenite affected the CPT, as shown in Fig. 6. Even when solution annealing was performed, there was a difference in the CPT. Moreover, the morphology of the heterogeneous austenite did not aid in increasing the CPT above 73 °C. When # f was subjected to solution annealing, which was uneven but had a difference in grain size, the CPT increased to 78.5 °C. The CPT was the highest at 83.4 °C in # e, where the morphology of austenite was the uniform from 7 μm to 23 μm.

It was confirmed that the morphology of austenite influenced the pitting corrosion. To improve the pitting corrosion resistance, the morphology of austenite in SDSS must be uniformly controlled.

### 3.3. Discussion

SDSS showed an improved pitting corrosion resistance after solution annealing; however, it exhibited differences in CPT based on the morphology and volume fraction of austenite before solution annealing [3-5]. When solution annealing was performed with the equal volume fractions, a decrease in CPT was observed. The ferritization of SDSS (55 %–70 % of the volume fraction of ferrite) improved the pitting corrosion resistance after solution annealing [8-15]. And that showed the best pitting corrosion resistance when it had uniform austenite.

**Table 5.** Grain size and volume fraction and morphology of austenite with and without solution annealing of super duplex stainless steel UNS S32750.

Diameter, μm	Austenite		Ferrite	
	Min	Max	Min	Max
# a, SA	4 ± 2	52 ± 15	2 ± 1	3 ± 1
# b, SA	3 ± 2	13 ± 2	2 ± 1	12 ± 9
# c, SA	4 ± 2	9 ± 3	2 ± 1	2 ± 1
# d, SA	5 ± 2	43 ± 8	5 ± 2	19 ± 5
# e, SA	7 ± 2	23 ± 4	0 ± 0	0 ± 0
# f, SA	3 ± 2	39 ± 5	2 ± 1	3 ± 1

The size of austenite in the specimens was measured, and the results are shown in Table 5 and Fig. 7. # c, SA had the uniform austenite sizes of 4–9  $\mu\text{m}$ , but it had a heterogeneous austenite morphology. # e, SA had a size of 7–23  $\mu\text{m}$  austenite, but it did not form fine ferrite. However, the morphology of austenite was uniform.

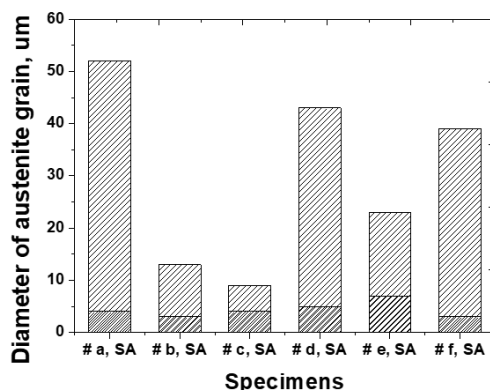


**Figure 7.** Diameter of austenite with volume fraction and morphology of austenite after solution annealing of super duplex stainless steel UNS S32750.

The pitting corrosion of SDSS is influenced by the chemical composition, but because CPT varies according to the morphology of austenite, the morphology of austenite must be uniformly controlled to optimize the corrosion resistance.

#### 4. CONCLUSION

The pitting corrosion resistance and effect of solution annealing on super duplex stainless steel were measured after controlling the morphology and volume fraction of austenite. The effects of the volume fraction and morphology of austenite in SDSS were investigated and compared as follows.

- 1) The volume fraction and morphology of austenite vary with the heat-treatment temperature and they can be controlled by heat treatment. The ferritization of SDSS developed a microstructure at 1200 °C, at which the austenite morphology became uniform. The volume fraction and morphology of the austenite were influenced by the solution annealing process.
- 2) The morphology of the austenite influenced pitting corrosion. When the morphology of austenite was spherical and the size was uniform at a range from 7 to 23  $\mu\text{m}$  (heat treatment at 1200 °C followed by solution annealing), it showed the best CPT (83.4 °C).
- 3) The pitting corrosion resistance of SDSS is affected by major alloys such as Cr, Mo, and N. However, it is mostly affected by the morphology of austenite according to heat treatment and processing conditions, which can be controlled by heat treatment conditions. Therefore, to optimize the

pitting corrosion resistance of SDSS, it is necessary to control the morphology of austenite by the temperature based on the process.

#### ACKNOWLEDGEMENT

This work was supported by the National Research Foundation of Korea(NRF) grant funded by the Korea government(MSIT) (No. 2020R1A5A8018822).

#### References

1. J. Kim, S. Choi, D. Park, and J. Lee, *Mater Des.*, 65 (2015) 914.
2. J. Jang, J. Ju, B. Lee, D. Kwon, and S. Kim, *Mater Sci Eng A.*, 340, 1–2 (2003) 68.
3. J. O. Nilsson, and A. Wilson, *J. Mater. Sci. Technol.*, 9 (1993) 545.
4. J. O. Nilsson, *J. Mater. Sci. Technol.*, 8 (1992) 685.
5. T. H. Chen, and J. R. Yang, *Mat. Sci. Eng. A-Struct.*, 311 (2001) 28.
6. C. J. Park, V. S. Rao, and H. S. Kwon, *Corrosion.*, 61 (2005) 76.
7. F. Iacoviello, F. Casari, and S. Gialanella, *Corros. Sci.*, 47 (2005) 909.
8. T. H. Chen, K. L. Weng, and J. R. Yan, *Mat. Sci. Eng. A-Struct.*, 338 (2002) 259.
9. M. Pohl, O. Storz, and T. Glogowski, *Mater. Charact.*, 58 (2007) 65.
10. C. P. Dias, and O. Balancin, *Metal. Mater. Trans., A*, 62 (2016) 155.
11. M. Martins, and L. C. Casteletti, *Mater. Charact.*, 60 (2009) 150.
12. J. M. Pardal, S. S. M. Tavares, M. C. Fonseca, J. A. de Souza, R. R. A. Corte, and H. F. G. de Abreu, *Mater. Charact.*, 60 (2009) 165.
13. E. Angelini, B. D. Benedetti, and F. Rosalbino, *Corros. Sci.*, 46 (2004) 1351.
14. H. Tan, Y. Jiang, B. Deng, T. Sun, and J. Xu, J. Li, *Mater. Charact.*, 60 (2009) 1049.
15. B. H. Shin, J. Park, J. Jeon, S. Heo, and W. Chung, *Anti-Corros. Methods mater.*, 65, 5 (2018) 492.
16. B. H. Shin, D. Kim, S. Park, J. Park, M. Hwang, and W. Chung, *Anti-Corros. Methods mater.*, 66, 1 (2019) 61.
17. Z. Wei, J. Laizhu, H. Jincheng, and S. Hongmei, *Mater. Charact.*, 60 (2009) 50.
18. N. J. Laycock, M. H. Moayed, and R. C. Newman, *J. Electrochem. Soc.*, 145 (1998) 2622.
19. M. B. Davanageri, N. S, and R. Kadoli, *AJMS.*, 5 (2015) 48.
20. J. L. Garin, and R. L. Mannheim, *International Centre for Diffraction Data*, (2012) 98.
21. S. H. Park, B. Shin, J. Park, D. Kim, and W. Chung, *Int. J. Electrochem. Sci.*, 14 (2019) 5386.
22. M. Youselieh, M. Shamanian, and A. Saatchi, *J. Alloys Compd.*, 509 (2011) 782.
23. S. S. M. Tavares, J. M. Pardal, L. D. Lima, I. N. Bastos, A. M. Nascimento, and J. A. de Souza, *Mater. Charact.*, 58 (2007) 610.
24. S. Wang, Q. Ma, and Y. Li, *Mater. Des.*, 32 (2011) 813.
25. M. Rahmani, A. Eghlimi, and M. Shamanian, *J. Mater. Eng. Perform.*, 23 (2014) 3745.
26. B. L. S. Lopes, S. F. Rodrigues, E. S. Silva, J. C. Damascena, V. S. Leal, *Materials Sciences and Applications*, 9 (2018) 228.
27. H. Y. Ha, M. H. Jang, T. H. Lee, J. O. Moon, *Corros. Sci.*, 89 (2014) 154.
28. Y.S. Ahn and J.P. Kang, *Mater. Sci. Technol.*, 16, 4 (2000) 382.
29. A. Belfrouh, C. Masson, D. Vouagner, A. M. de Becdelievre, N. S. Prakash, J. P. Audouard, *Corros. Sci.*, 38, 10 (1996) 1639.
30. C. W. Hsu, T.E. Chen, K.Y. Lo, Y. L. Lee, *APL Mater.*, 12 (2019) 307.